Vesicles

DOI: 10.1002/ange.201100410

A Theta-Shaped Amphiphilic Cobaltabisdicarbollide Anion: Transition From Monolayer Vesicles to Micelles**

Pierre Bauduin, Sylvain Prevost, Pau Farràs, Francesc Teixidor, Olivier Diat, and Thomas Zemb*

Self-assembly is ubiquitous in nature and in surfactant science.[1] Globular micelles or vesicles in water are usually obtained with surfactants[2] or amphiphilic block copolymers[3] composed of a hydrophilic part and a hydrophobic part. The aggregation mechanism is then controlled by the tendency of the nonpolar part to avoid contact with water, known as the hydrophobic effect,[4] while the polar part tends to be strongly hydrated. Consequently, the minimum free energy is reached during the aggregation process by minimal contact of the hydrocarbon chains with water and by maximal entropy that lead to the formation of the smallest possible aggregates, that is, spherical micelles for single-chain surfactants. As the concentration increases, the shape changes from spherical micelles to rods (hexagonal phase) to a lamellar phase, that is, from high to low curvature toward the apolar part.[5] Double-chained surfactants, or some block copolymers with a pronounced hydrophobic tendency, cannot pack into spheres because of steric reasons, and are forced immediately into closed bilayers (vesicles) of near-zero curvature at the surfactant/copolymer scale.[6] Recently, the formation of vesicles has been reported for more exotic, that is, non-amphiphilic chemical systems such as amino acid derivatives, oligopeptides, cyclodextrins, macrocycles, fluorofullerenes, and polyelectrolytes.[7]

Herein we show that the cobaltabisdicarbollide (mono-) anion $(H^+[3,3'\text{-}Co(1,2\text{-}C_2B_9H_{11})_2]^-$ (H^+COSAN^-; Figure 1) forms monolayer vesicles at low concentrations in water. An increase in concentration leads to a phase transition from vesicles to small micelles (Figure 1) and results in the coexistence of both aggregation states at higher concentrations. The formation of monolayer vesicles and small micelles was hitherto unknown for water-soluble carborane derivatives.

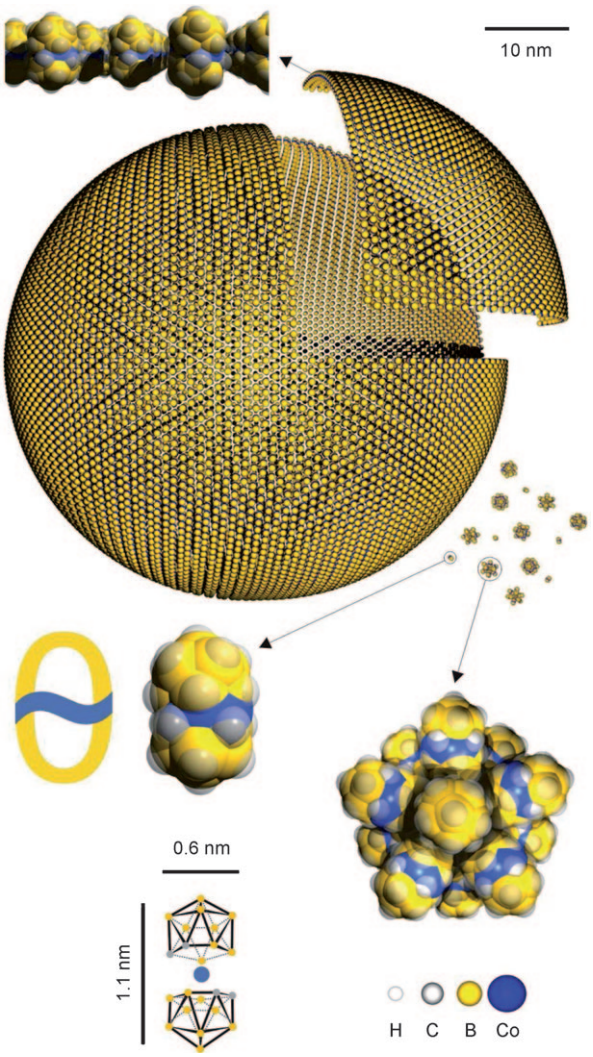

Figure 1. The cobaltabisdicarbollide anion ($COSAN^-$, $[(C_2B_9H_{11})_2Co]^-$) is composed of two bulky and hydrophobic dicarbollide semicages (yellow) that "sandwich" a cobalt(III) ion as the polar part (blue). Hydrogen atoms are omitted for clarity in the crystal structure.

COSAN is composed of two bulky and highly hydrophobic dicarbollide semicages, each of them bearing two negative charges, that "sandwich" a cobalt(III) ion as the polar part. The remaining negative charge is delocalized over the entire COSAN structure that can be represented by the Greek letter θ (see Figure 1). COSAN is used in its acidic form, with a proton (H^+) as counterion. Titration with a strong base shows that HCOSAN acts as a strong acid (see the Supporting Information), hence it is charged and fully dissociated in water. This species shows high solubility in water and a monotonic surfactant-like reduction of water

[*] Dr. P. Bauduin, Dr. O. Diat, Prof. T. Zemb
ICSM, UMR 5257 (CEA, CNRS, UM2, ENSCM)
CEA Marcoule, BP 17171, 30207 Bagnols-sur-Cèze (France)
Fax: (+33) 4-6679-7611
E-mail: pierre.bauduin@cea.fr
Dr. S. Prevost
HZB (Helmholtz-Zentrum Berlin) für Materialien und Energie and Stranski Laboratory and Technische Universität Berlin
Strasse des 17. Juni 124, 10623 Berlin (Germany)
Dr. P. Farràs, Prof. F. Teixidor
ICMAB CSIC, Campus de la UAB, 08193 Bellaterra (Spain)

[**] We thank Dr. Emma Rossinyol (Servei de Microscòpia Electrònica de la UAB) for valuable assistance with the cryo-TEM studies and Dr. Fabienne Testard (CEA Saclay DSM/IRAMIS/SIS2M/LIONS) for fruitful discussions.

Supporting information for this article is available on the WWW under http://dx.doi.org/10.1002/anie.201100410.

surface tension.[8] As can be seen in Figure 1, because of the charge and θ shape of the COSAN anion, counterions can neither approach it closely enough to reduce the Born energy, nor can the hydrophobic rigid ends deform to partition on one side of the head group as in double-tailed surfactants. These two peculiarities lead to the formation of unique microstructures.

COSAN aggregation was characterized by combining small- and wide-angle X-ray and neutron scattering (SAXS, WAXS, and SANS) in D_2O at concentrations ranging from 0.0065 to 1.127 M (0.19 to 33.3% v/v). Figure 2a shows the SANS spectra for concentrations of 0.0065 and 1.127 M. The SANS intensity is plotted as a function of the wave vector q, defined as $q = 2\pi/\lambda \sin(\theta/2)$ where θ is the scattering angle. For the very dilute sample, a strong increase in intensity at low q values is observed, which is characteristic of large heterogeneities ($2\pi/q > 10$ nm). For concentrations above 20 mM (0.5% v/v), a correlation peak appears at larger q values, typical of small interacting colloids (in the nanometer range), in addition to the low q signal. Two types of COSAN aggregates, large and small, are thus formed successively as the concentration increases. Similar conclusions can be drawn from SAXS measurements.

By using a spherical shell model for the large (vesicle-like) aggregates and a dense sphere model for the small ones (globular micelles), the SANS spectra can be described over the whole concentration range in a logarithmic scale (see Figure 2a and the Supporting Information). In addition, the contributions of the micelles (– – –) and the vesicles (•••••) to the total scattered intensity are given separately. For 0.0065 M (□), only the vesicles contribute to the scattered intensity as no micelles are present in the solution.

For vesicles, a radius $R_{vesicle}$ of approximately 20 nm is derived from the SANS data over the available q range. Information on the vesicle sizes is also obtained from static light scattering in the very low concentration range from 0.02 to 0.69 mM (i.e. 5.9×10^{-4} to 2.0×10^{-2}% v/v), where only vesicles are present in solution. The vesicle radius ($R_{vesicle} = (19\pm1)$ nm) is determined from the calculation of the aggregation number of the vesicle, $N_{agg.}^{vesicle} = (12500\pm100)$. In addition, plotting the scattered light intensity vs. the COSAN concentration gives access to the critical aggregation concentration, $cac_{vesicle} \approx 0.01$ mM, which corresponds to the monomer-to-vesicle transition. Such low aggregation concentrations are common for vesicle-forming surfactants, polymers, or for example, doubled-chained surfactants such as phospholipids.

For the micelles, a radius R_{mic} of 1.16 nm (approximately the length of a COSAN molecule) is obtained, hence indicating that small globular micelles with an aggregation number of approximately 14 are formed (Figure 1). A subtle increase in the micelle concentration (n_{mic}), which results from the fit, is observed at a COSAN concentration of 18.6 mM, that is, $\phi_{cac}^{mic} = 0.54$% (see the Supporting Information), which corresponds to the critical aggregation concentration of the micelles (cac_{mic}). Above cac_{mic}, micelles begin to form, thus leading to their coexistence with the vesicles.

The thickness of the vesicle shell (ΔR) was determined from the scattering curve at 0.19% v/v (where only the vesicles

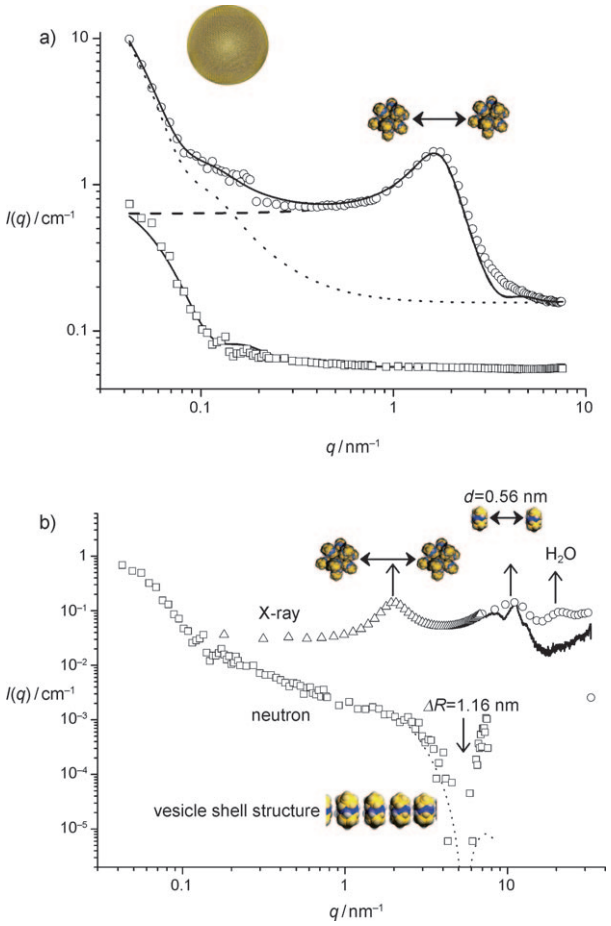

Figure 2. a) SANS spectra of HCOSAN in D_2O at 0.19 (□) and 33.3% v/v (○). Solid lines represent the best fit obtained by combining two populations of spherical objects: 1) vesicles with polydisperse radius (25 nm) and constant wall thickness (1.16 nm), and 2) spherical micelles of 1.16 nm radius that interact through a hard-sphere potential. The contributions of the micelles and the vesicles to the total scattered intensity are given separately as dashed and dotted lines respectively. b) SANS spectrum (□) of HCOSAN in D_2O at 0.19% v/v after subtraction of the background. The dotted curve is a simulation in absolute scale of infinite lamella with a wall thickness of 1.16 nm. SAXS (△) and WAXS (○) spectra of HCOSAN at 33% v/v. At high q values, the spectrum (solid line) corresponds to the WAXS spectrum (in arbitrary units) of pure HCOSAN powder.

are present) by using an expression for the scattered intensity in absolute scale of infinite lamella (see the Supporting Information).[9] The first oscillation in the scattered intensity, observed in the q range 2.4–7 nm^{-1} after subtraction of the background contribution (see Figure 2b), is well reproduced by this model for a wall thickness of 1.16 nm corresponding to the length of a COSAN ion (dotted line in Figure 2b). The shell is then formed by a COSAN monolayer with the COSANs oriented orthogonally to the shell surface as shown in Figure 1 and Figure 2b. This is an outstanding feature of COSAN vesicles compared to "conventional" vesicles of comparable size made from surfactants. For those systems, the shell is formed by a bilayer that prevents the contact of the hydrophobic tails with water.

As HCOSAN is fully dissociated in water, electrostatic repulsions between COSAN ions must be substantial. To

study the influence of the electrostatic interactions on the aggregation, NaCl was added to a solution containing vesicles ([HCOSAN] = 3.7 mM). The size of the vesicles as a function of NaCl concentration was investigated by dynamic light scattering (DLS; see the Supporting Information). After addition of NaCl, a large increase in the hydrodynamic diameter from 80 to 890 nm is observed. This result confirms that electrostatics play an important role in the COSAN aggregation process. Thus, the aggregation of COSAN in water results from a subtle combination of electrostatic, hydrophobic, and dispersion forces.

Focusing on a larger q range, WAXS experiments (○, Figure 2b) reveal the presence of two other broad interaction peaks. The peak at higher q values corresponds to the liquid order of water and is not of interest here. Another peak is observed at 10.8 nm^{-1}, which is characteristic of the closest accessible Co–Co distance ($d = 2\pi/q = 0.56$ nm) between two COSANs in aggregates. From molecular modeling (Figure 1), the shape of the COSAN molecule can be approximated by a biaxial ellipsoid with the Co atom at the center and can be characterized by a main axis of about 1.1 nm and a semiaxis of about 0.6 nm. For comparison, this liquid-order correlation peak is at the same q value as the main Bragg peak observed in the WAXS spectrum of pure HCOSAN powder; thus it can be concluded that COSAN ions are at close contact and in a liquidlike state in the aggregates.

To validate this unusual sequence of shapes observed by combined X-ray, neutron, and light scattering, cryo-TEM was performed on a sample at a concentration above cac_{mic} (Figure 3). Cryo-TEM confirms the sizes of the micelles and vesicles as well as their coexistence (Figure 3a). The hollow structure of the vesicles inferred from the SANS data could also be evidenced (Figure 3b).

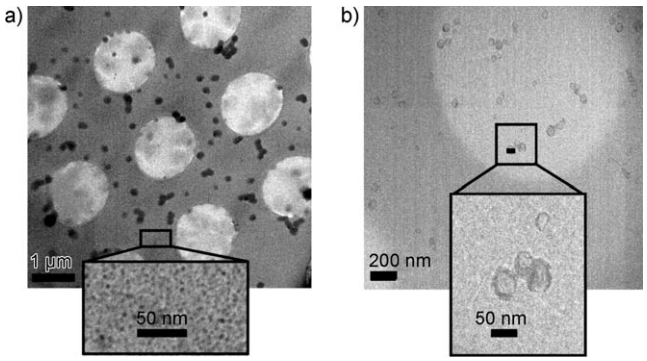

Figure 3. Cryo-TEM images of HCOSAN in H_2O at 33 %v/v show: a) The presence of small globular micelles of about 2 nm that coexist with larger vesicle-like aggregates, and b) the hollow structure of the vesicle-like aggregates that are about 50 nm in diameter. In both images the large bright circles are the holes in the TEM grid.

The unconventional aggregation behavior of COSAN originates from the combination of its θ-shape amphiphilic structure, charge density, and rigidity. This leads to unexpected properties of COSAN derivatives that might be interesting for applications, such as selective ion pairing used in the reprocessing of spent nuclear fuel,[10] as main component in ion-selective electrodes,[11] or as HIV-protease inhibition.[12] Indeed, COSAN and its derivatives have been proposed lately as novel nonpeptide enzyme inhibitors for rational drug design. The multi-scale self-assembly of COSAN is also of potential interest in materials science. In most of these applications, COSAN derivatives are dissolved in water, in which aggregation properties may play a crucial role. A better understanding of the aggregation process would be helpful for the design and optimization of these applications.

Received: January 17, 2011
Revised: March 29, 2011
Published online: May 11, 2011

Keywords: carboranes · cryo-TEM · micelles · small-angle neutron scattering · vesicles

[1] D. F. Evans, H. Wennerström, *The Colloidal Domain: Where Physics, Chemistry, Biology, and Technolody Meet*, Wiley-VCH, Weinheim, **1999**.
[2] K. Holmberg, B. Jonsson, B. Kronberg, B. Lindmann, *Surfactants and Polymers in Aqueous Solution*, Wiley-VCH, Weinheim, **2002**.
[3] L. Zhang, A. Eisenberg, *Science* **1995**, *268*, 1728 – 1731.
[4] a) C. Tanford, *The Hydrophobic Effect: Formation of Micelles and Biological Membranes*, Wiley, New York, **1973**; b) D. Chandler, *Nature* **2005**, *437*, 640 – 647.
[5] S. Hyde, S. Andersson, K. Larsson, Z. Blum, T. Landh, S. Lidin, B. W. Ninham, *The language of shape*, Elsevier, Amsterdam, **1997**.
[6] a) M. Dubois, B. Demé, T. Gulik-Krzywicki, J. C. Dedieu, C. Vautrin, S. Désert, E. Perez, T. Zemb, *Nature* **2001**, *411*, 672 – 675; b) M. Gradzielski, *J. Phys. Condens. Matter* **2003**, *15*, 655 – 697; c) E. W. Kaler, A. K. Murthy, B. E. Rodriguez, J. A. N. Zasadzinski, *Science* **1989**, *245*, 1371 – 1374; d) M. Antonietti, S. Förster, *Adv. Mater.* **2003**, *15*, 1323 – 1333; e) H. Shen, A. Eisenberg, *Angew. Chem.* **2000**, *112*, 3448 – 3450; *Angew. Chem. Int. Ed.* **2000**, *39*, 3310 – 3312.
[7] a) T. Homma, K. Harano, H. Isobe, E. Nakamura, *Angew. Chem.* **2010**, *122*, 1709 – 1712; *Angew. Chem. Int. Ed.* **2010**, *49*, 1665 – 1668; b) F. Rodler, J. Linders, T. Fenske, T. Rehm, C. Mayer, C. Schmuck, *Angew. Chem.* **2010**, *122*, 8929 – 8932; *Angew. Chem. Int. Ed.* **2010**, *49*, 8747 – 8750; c) H. S. Seo, J. Y. Chang, G. N. Tew, *Angew. Chem.* **2006**, *118*, 7688 – 7692; *Angew. Chem. Int. Ed.* **2006**, *45*, 7526 – 7530; d) M. Reches, E. Gazit, *Science* **2003**, *300*, 625; e) B. J. Ravoo, R. Darcy, *Angew. Chem.* **2000**, *112*, 4494 – 4496; *Angew. Chem. Int. Ed.* **2000**, *39*, 4324 – 4326; f) D. Volodkin, Y. Arntz, P. Schaaf, H. Moehwald, J. C. Voegel, V. Ball, *Soft Matter* **2008**, *4*, 122 – 130.
[8] A. Popov, T. Borisova, *J. Colloid Interface Sci.* **2001**, *236*, 20 – 27.
[9] L. Cantú, M. Corti, E. Del Favero, M. Dubois, Th. Zemb, *J. Phys. Chem. B* **1998**, *102*, 5737 – 5743.
[10] G. Chevrot, R. Schurhammer, G. Wipff, *J. Phys. Chem. B* **2006**, *110*, 9488 – 9498.
[11] a) A. L. Stoica, C. Vinas, F. Teixidor, *Chem. Commun.* **2008**, 6492 – 6494; b) A. L. Stoica, C. Vinas, F. Teixidor, *Chem. Commun.* **2009**, 4988 – 4990.
[12] P. Cigler, M. Kozisek, P. Rezacova, J. Brynda, Z. Otwinowski, J. Pokorna, J. Plesek, B. Grüner, L. Doleckova-Maresova, M. Masa, J. Sedlacek, J. Bodem, H. Kräusslich, V. Kral, J. Konvalinka, *Proc. Natl. Acad. Sci. USA* **2005**, *102*, 15394 – 15399.

